www.elsevier.com/locate/ijmecsci

Depth-dependent stress-strain relation for friction prediction

Muhammad Taureza, Xu Song, Sylvie Castagne

PII: S0020-7403(14)00046-0
DOI: http://dx.doi.org/10.1016/j.ijmecsci.2014.02.006
Reference: MS2637

To appear in: *International Journal of Mechanical Sciences*

Received date: 28 June 2013
Revised date: 24 January 2014
Accepted date: 8 February 2014

Cite this article as: Muhammad Taureza, Xu Song, Sylvie Castagne, Depth-dependent stress-strain relation for friction prediction, *International Journal of Mechanical Sciences,* http://dx.doi.org/10.1016/j.ijmecsci.2014.02.006

Depth-dependent stress-strain relation for friction prediction

Muhammad Taureza[a], Xu Song[b], Sylvie Castagne[a,*]

[a] School of Mechanical and Aerospace Engineering, Nanyang Technological University, Singapore, Singapore

[b] Forming Technology Group, Singapore Institute of Manufacturing Technology, Singapore, Singapore

[*] Corresponding author:

Telephone : (65) 6790 4331

Fax : (65) 6792 4062

E-mail address : scastagne@ntu.edu.sg

Postal address : Nanyang Technological University, School of Mechanical and Aerospace Engineering, 50 Nanyang Avenue, N3.2-02-17, Singapore 639798

Abstract

The effect of strain gradient on mechanical property of material is implemented through depth-dependent stress strain relation model in conventional finite element simulations for use in friction prediction. For the incorporation of strain gradient effect, contact simulation involving asperities was developed with the assumption that the deformation pattern created by asperities from tool surface in microforming is comparable to the deformation created by the indenter in a hardness test. Consequently, depth-dependent stress-strain relation was derived from the indentation size effect model and this stress-strain relation was used in a simulation to show the effect of strain gradient to friction behaviour in microforming at different surface roughness levels. Experiment was conducted alongside the simulation and the results showed that with asperity ploughing considered as major contributor to friction in microforming at room temperature, the simulation involving depth-dependent material properties is able to predict the better predict the friction behaviour as compared to its continuum simulation counterpart.

Keywords

Asperity interaction, indentation size effect, strain gradient effect, friction simulation

1. INTRODUCTION

Current technologies have been developed through and around the development of miniaturization techniques. IT, technology hardware and process automation for micro-processes are examples of industries which have benefited from the knowledge towards miniaturization. At the present, the production of micro-parts has been dominated by micro-machining and MEMS-based techniques such as ion beam and electron beam lithography. Because of the merits of producing parts to the near-net shape at high volume and for minimum waste, metal forming processes continues to be developed to stretch their limits to produce smaller components to the sub-millimetre scale, known as microforming [1].

The design of metal forming processes has been aided greatly by the development in 2D and 3D Finite Element (FE) simulation. In a typical FE simulation, users need to provide the material properties (mechanical, thermal, etc.) and the interfacial conditions (friction, heat transfer) for the analysis code to provide predictions such as die stresses as well as strain and damage distribution inside the deforming component.

One major challenge in miniaturizing metal forming processes is that the knowledge in macro metal forming is not always transferrable to microforming, i.e. the material properties and interfacial conditions are different. The shift of behaviours in microforming, known as size effects, has been well documented [1, 2] and categorized [3, 4].

For conventional metal forming processes, the FE simulation generally uses the continuum material model where the stress (σ) can be described as a function of the strain (ε), the strain rate ($\dot{\varepsilon}$) and the temperature (T). However, for smaller size deformation, various simulation approaches have been attempted such as the crystal plasticity simulation [5, 6] and the gradient-dependent plasticity simulation [7, 8] in order to provide better process prediction.

This paper proposes an approach to account the effect of strain gradient to mechanical properties of materials [9] which contributes to the size effects using finite element simulation through a modified continuum model in order to avoid performing the more computationally-exhaustive crystal plasticity or gradient-dependent plasticity simulation for use in microforming prediction. With the inclusion of strain gradient model, the mechanical properties of materials at and near the surface is significantly affected, resulting in shift in surface behaviour. While this shift of surface behaviour is not large enough to influence the overall process behaviour in metal forming, the process behaviour in microforming with much smaller workpieces is significantly affected due to the larger surface area to volume ratio.

In a previous study with conical asperity [10], it was shown that the measured friction during the simulation is lower when the depth-dependent flow stress is introduced. More importantly, the influence of indentation size effect model is stronger in smoother surface. The current study aims to develop further the depth-dependent flow stress model and provide validation to the strain gradient friction model.

2 SIMULATION

2.1 Indentation size effects

Along with the growing interest in recent years for micro- and nano-structures such as thin films, micro-wires, flexible electronics and fibre composites, there is increasing interest in understanding the mechanical properties of materials at very small scale. Experiments in micro- and nano-indentation test have revealed the dependency of material hardness on the size [9] and shape [11] of the indentation. Nix and Gao [9] proposed a mechanism-based model (Equation 1) which agrees to micro-indentation results by considering the

development of geometrically necessary dislocations (GND) and statistically stored dislocation (SSD) during deformation by a conical indenter. In the model, the hardness at the indentation depth of interest (H) can be related to the indentation depth (h) through experimentally determined constants of the bulk hardness (H_0) and the material length scale (h^*) which are material dependent.

$$\frac{H}{H_0} = \sqrt{1 + \frac{h^*}{h}} \tag{1}$$

This phenomenon is known as the Indentation Size Effect (ISE) and linked to strain gradient plasticity. However, experimental results from nano-indentation at very small indentation depth have shown significant deviation from the model of Nix and Gao. Consequently, models have been proposed to account and explain this deviation using different indenter geometries, at different indentation depths and with different materials [12-14]. In general, the hardness at shallow indentation (using nano-indentation tests) is lower than the value suggested by Nix and Gao.

Qiu et al. [15] proposed that when dislocation is considered, the effect of material friction stress (τ_0) should not be ignored and the complete Taylor's equation of flow stress (equation 2) should be considered. In equation 2, μ and b are shear modulus and Burgers vector, α is a proportionality constant and ρ is the dislocation density (SSD and GND). The material friction stress was not considered in Nix and Gao model as the materials in observation were copper and silver. However, for BCC metals and other materials with strong covalent bonds, the material friction stress is significant. Equation 2 essentially separates the flow stress from dislocation from those otherwise. As a result, the ISE equation from Qiu et al. [15] contains a threshold hardness value related to the flow stress not attributed to dislocation generation (denoted Y, Equation 3). It was proposed that for FCC metals, the Y should be negligible and

hence the equation reverts to Equation 1.

$$\tau = \alpha\mu b\sqrt{\rho_S + \rho_G} + \tau_0 \tag{2}$$

$$\frac{H - Y}{H_0} = \sqrt{\left(\frac{H - Y}{H}\right)^2 + \frac{h^*}{h}} \tag{3}$$

The size of the plastic zone was further studied in the work by Feng and Nix [14]. This deviation has been attributed to a difference in formation and arrangement of GND and SSD from very small deformation in nano-indentation test. The motivation for the work was to provide other explanation for the lower hardness at very shallow indentation. The explanation by Qiu et al [15] was considered inadequate by Feng and Nix [14] as the lower hardness at very shallow indentation applies not only to BCC metals but also in FCC metals. A coefficient which represents plastic zone growth, f (Figure 1), was included into the ISE equation (Equation 4). It was also determined that the plastic zone can grow up to 66% larger (f = 1.66) than the contact for MgO at the surface ($h \rightarrow 0$) and 71% (f = 1.71) for iridium (FCC metal) [14].

$$\frac{H}{H_0} = \sqrt{1 + \frac{h^*}{f^3 h}} \tag{4}$$

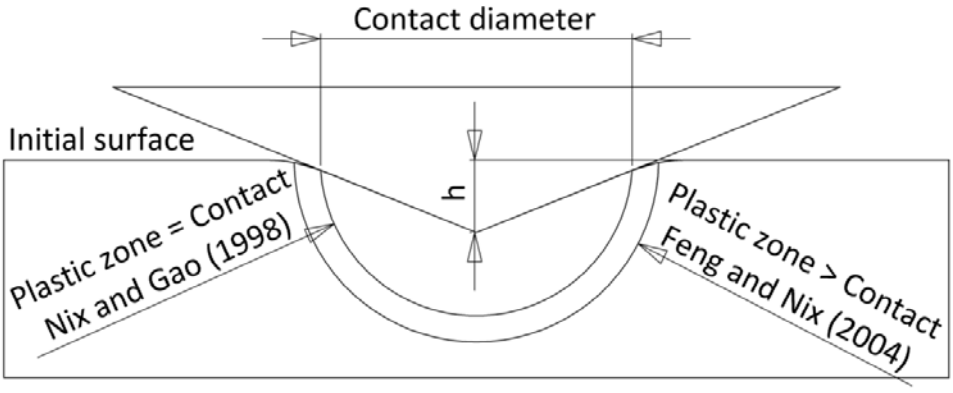

Figure 1: Plastic zone growth

Chicot [13] proposed a bi-linear equation to treat micro-indentation and nano-indentation separately. In the model, micro- and nano-indentation regimes were treated using two separate Nix and Gao type equations. Each regime was then assigned different values of H_0 and h^* to fit the experimental results for the entire range of the indentation tests. The two indentation regimes were further proposed to be renamed as uniform dislocation spacing (UDS) and non-UDS regimes for micro- and nano-indentation, respectively. In the micro-indentation, the plastic zone (zone of GND development) diameter is equal to the contact diameter. The same does not apply in nano-indentation or non-UDS regime. However, the bi-linear equation was proposed with inadequate physical explanation for the difference in constants for the two regimes.

The model of Abu Al-Rub [16] has been proven reliable to predict the ISE of various metals through micro- and nano-indentation experiments and it includes physical meaning of variables as have been considered in previous studies. It is therefore used in the current investigation. In general, Abu Al-Rub model considers both a threshold hardness value as well as the growth of plastic zone. In addition, similar to the observation by Feng and Nix, the growth of the plastic zone was also related to the indentation size (or depth) through the dislocation coupling coefficient, β. The main difference between Nix-Gao and Abu Al-Rub model is presented in Table 1. The present work treats surface asperities of metal forming tool as indenters in hardness testing.

Table 1: ISE formulae of Nix-Gao and Al-Rub

	Nix and Gao [9]	**Abu Al-Rub [16]**
ISE Formula	$\frac{H}{H_0}=\sqrt{1+\frac{h^*}{h}}$	$\frac{H-Y}{H_0-Y}=\sqrt[\beta]{1+\left(\frac{h^*}{h}\right)^{\beta/2}}$

2.2 Simulation setup

Friction involves the presence of roughness convex and concaves on contacting surfaces, called asperities (Figure 2). This asperities distribution generally governs the real area of contact which is generally much smaller than the apparent area of contact [17]. The large number of asperities during surface to surface contact was then used to justify that the friction coefficient during continuous sliding can be attributed to the averaged behaviour of the interaction between asperities, from initiating contact to deformation to separation. Green [18] used this assumption to develop the basis of friction simulation involving asperities in which friction can be modelled using two asperities (one from each surface) undergoing the full cycle of asperity interaction (initiating contact to deformation to separation). The averaged tangential and normal forces derived from this simulation were therefore extracted as the frictional properties.

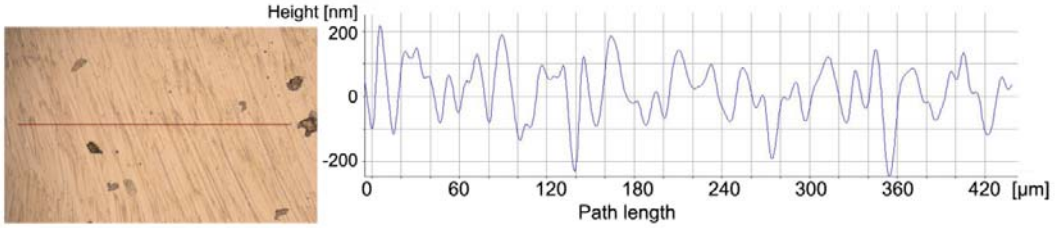

Figure 2: Surface profile of the polished steel pin

This modelling approach is valid with the assumption of uniformity among asperities including their mechanical properties. Mulvihill et al. [19] provided good summary on the development of researches on friction simulation using this approach. However, the modelling approach has a setback: the resulting friction predicted from the simulation generally suggests values which are much lower compared to experimental results from metal to metal contacts. In order to generate simulation results in better agreement with

experiments, researchers generally used the Coulomb friction coefficient to offset for the higher friction observed in experiments. Such incorporation of Coulomb friction coefficient as additional friction definition in order to offset the simulation results is generally inaccurate as the Coulomb friction law was derived from macroscopic experiment whereas the microscopic simulation using asperities was initiated to understand the mechanism of macroscopic friction.

Instead of using the averaged transient process of contact initiation to deformation to separation, the simulation in the current work uses steady state sliding of two surfaces with appropriate material definition to generate the friction behaviour. As the current investigation is aimed to address medium to high contact pressure problems such as those occurring in metal forming, the simulation work was designed to use single-sided asperity contact. The harder surface during metal forming contact, the tool, was prescribed with one asperity while the workpiece was represented by a smooth surface. This configuration is adequate for metal forming purpose as the workpiece surface is usually much softer than the tool surface. In which case, the workpiece will copy the surface roughness of the tool.

Generally, at medium to high pressure contact during metal forming, the two materials can have a full contact in which the real contact area equals the apparent contact area [20] and therefore the final surface profile (after contact) of the workpiece is more important than the initial surface profile (before contact) and the definition of asperities on the workpiece surface has little meaning.

The yield stress of a material is generally accepted to be proportional to its hardness, with the proportionality constant (x in Equation 5) varies from 2.5 to 3.0 for most metals.

Tabor [21] suggested a method to construct stress-strain relation from a series of hardness

testing by assuming the true strain during indentation as proportional to d/D, with d the contact diameter and D the ball diameter for spherical indenter (Equation 6) if the strain hardening exponent, n, is known. However, implementing this conversion is not possible because: a) increasing d/D to get larger strain would result in increasing indentation depth, which is known to affect the measured hardness, and b) the maximum d/D is limited to 1 which is equivalent to a true strain of 0.2.

$$H = x\sigma \tag{5}$$

$$p \approx 3\sigma_y \left(0.2\frac{d}{D}\right)^n \tag{6}$$

As there is no systematically established method to create the stress-strain relation over large range of strain from hardness testing, the current study assumes that the bulk of the workpiece has the property of a typical copper material represented in Figure 3. This stress-strain relation is further multiplied by the depth-dependent coefficient H/H_0 presented in Figure 4 to create the depth-dependent flow stress of the material ($\sigma(\varepsilon,h)$, Equation 7).

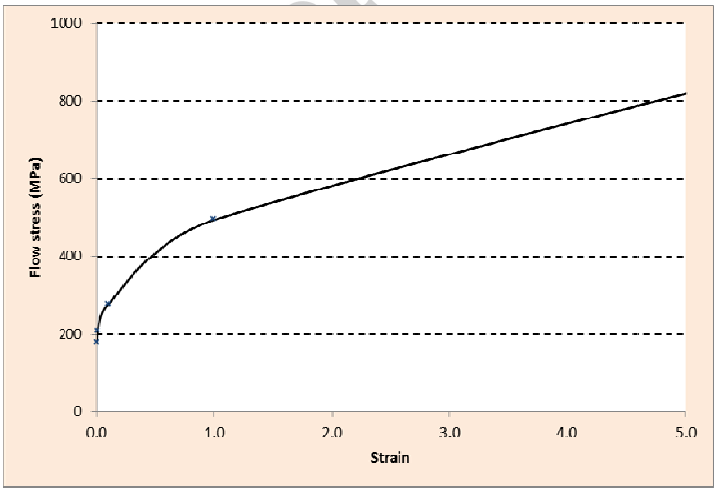

Figure 3: Stress-strain relation used in simulation

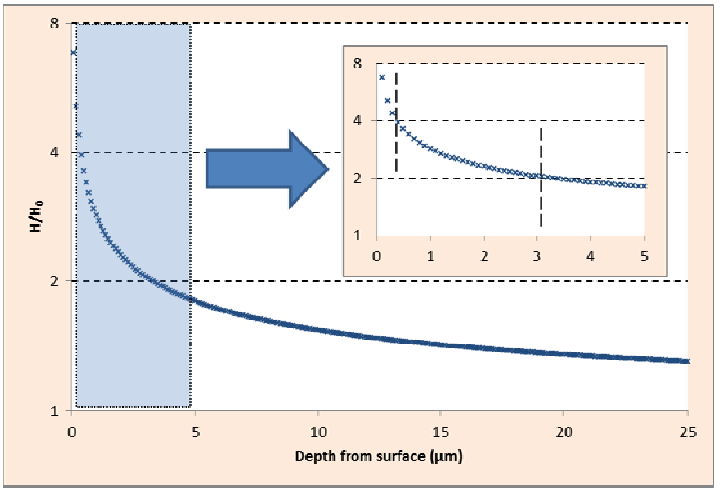

Figure 4: Depth-dependent stress-strain relation coefficient

$$\sigma(\varepsilon,h)=\sigma(\varepsilon)*\frac{H}{H_0}(h) \tag{7}$$

The depth-dependent coefficient was derived using the ratio between the measured hardness and the bulk hardness, H/H_0, from the work by Abu Al-Rub [16] for copper (Figure 4). The work reveals that the relative hardness (H/H_0) doubles at approximately 3 µm from the surface. The effect exponentially increases for region nearer to the surface with the relative hardness quadruples at approximately 0.4 µm. The mechanical properties for the first 3 µm from the surface is highly important with respect to friction as it is within range of naturally formed asperity size from surfaces made through machining processes and polishing.

The interaction between the tool and workpiece was specified as frictionless since adhesive friction is ignored in the current examination. Adhesive friction can be included by considering micro-welds formation during contact and can be included through fixed shear strength which corresponds to the stress required to break the micro-welds. However, the appropriate magnitude of the fixed shear strength can only be determined empirically by

comparing experimental results with simulation with various fixed shear strength.

In the simulation, 3D workpiece domain adapted from the 2D friction reading mesh of Stupkiewicz [22] as illustrated in Figure 5 was used to investigate the influence of surface roughness on sliding friction.

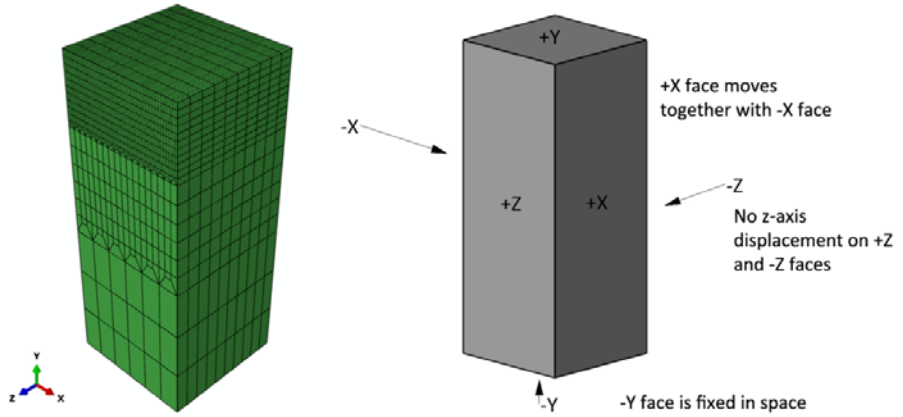

Figure 5: Full workpiece material mesh and assignment of faces

The tool surface in the simulation (Figure 6) is designed to have a periodic array spherical asperity with the period of 10 µm in x- and z-direction. Because of the assumed periodicity, the simulation domain is selected as 10 x 10 µm with the necessary periodic boundary conditions applied. The simulation domain has a thickness of 25 µm and this thickness is considered adequate for good representation of the DSS relation as it covers the range of depths with steep H/H_0 gradient (Figure 4).

The level of surface roughness is created by changing the radius of the spherical asperity (Table 2). The surface roughness used in this simulation was approximately Sa 0.5, 1.0 and 2.5 µm representing polished surface, ground surface and rough surface respectively. Areal roughness parameter, Sa, was used instead of the more common linear roughness parameter, Ra, in order to provide better definition for the whole area of contact in the simulation. Inclusion of other surface profile parameters (e.g. skewness, kurtosis, density of asperities)

would create more accurate representation of actual surfaces. However, this inclusion requires larger simulation mesh to constitute representative volume elements and this was not the focus of the current study.

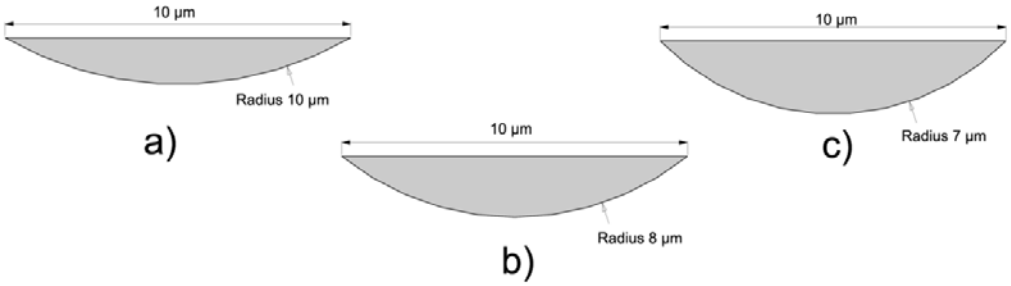

Figure 6: Tool material domain for: a) Sa 0.5, b) 1.0 and c) 2.5 µm

Table 2: Conversion of surface roughness to asperity radius

Surface roughness (Sa, µm)	**Equivalent spherical asperity radius (µm)**
0.5	10
1.0	8
2.5	7

Finite element code Abaqus was used for the modelling. Due to the demanding contact calculations, the Abaqus/Explicit was used. The simulation used linear hexahedral elements with reduced integration for the workpiece and rigid body elements for the tool. Both bodies are prescribed with concentrated elements surrounding the contact area. The temperature degree of freedom was used to provide *pseudo* temperature-dependent mechanical properties to describe mechanical properties at different depth from the surface. Prior to the analysis step, the workpiece mesh was prescribed heat and cold sink boundary conditions and it was allowed to generate constant gradient of temperature across the thickness Figure 7. In this simulation, the region closer to the surface is set with cold sink boundary condition representing the harder volume due to the depth-dependent coefficient and the region farthest

from the surface is set with heat sink boundary condition representing the softer volume (material property leaning towards the bulk material).

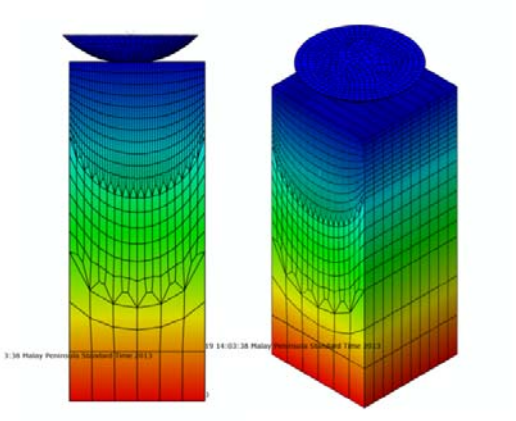

Figure 7: Temperature gradient (NT11 variable) fully develops across domain thickness

In the simulation, the workpiece mesh was pinned at the bottom (-Y face). The periodic boundary condition was prescribed using zero-translation boundary condition at the +Z and -Z faces and using tie constraints at every mirroring nodes at the +X and -X faces such that the translation field in all three directions experienced at the +X face is also experienced at the -X face. The contact pressure was produced by moving the tool into the workpiece (-Y direction). Afterwards, the tool is prescribed with a sliding movement parallel to the workpiece surface (+X direction) and the reaction forces along X and Y directions were recorded to produce normal and friction stresses. The simulation was repeated with a different displacement of the tool into the workpiece to provide prediction of friction behaviour at various contact pressures.

Tool steel pin on copper flat tribometer experiments were performed alongside the simulation to provide verification for the model. The pins are produced with circular contact of 1 mm diameter. The small contact diameter was necessary to reduce the tribometer load required to create high contact pressure which is the interest in metal forming. The pins were

supplied with two kinds of surface finish: polished and ground using 600-grit sand paper. The surface roughnesses of the pins are 0.4-0.5 μm and 0.9-1.0 μm, for polished and ground pins respectively.

The tribometer experiment is conducted at room temperature and ambient humidity (80-95%). The simulation considers solely the friction behaviour during ploughing friction without the presence of third body particles or friction heating. In order to produce the most representative experiment to this simulation, the experiment in this study involves only a one-time sliding on fresh samples with sliding speed approximately 0.1 mm/s. The one-time sliding is chosen as repetitive sliding between surfaces is likely to produce third body particles through surface shearing and sub-surface cracking [23, 24]. Slow sliding speed further minimizes the production of heat on the surface due to friction [25] which is not currently considered in the simulation.

3 DISCUSSION

Figure 8 shows the simulation results using DSS model for Sa 1.0 μm and tribometer experiment using ground pin. Figure 8 showed an increase of coefficient of friction with increasing contact pressure which is in agreement with the observation of Mulvihill et al. [19] in which the coefficient of friction increases with the amount of asperity overlap. In the current study, the changing contact pressure was obtained by introducing a known deformation depth from the asperity, which is equivalent to the asperity overlap in the simulation works inspired by Green.

Unlike the simulation results, experiments do not result in an increase of friction with contact pressure. This can be explained because the current simulation was aimed specifically to examine the influence of the DSS relation on friction based on asperity deformation

mechanism whereas friction in experiments also includes aspects such as adhesion and steady-state surface degradation. The large error bar in the experimental results for ground pin is attributed to the significant stick-slip behaviour between the pin and plate.

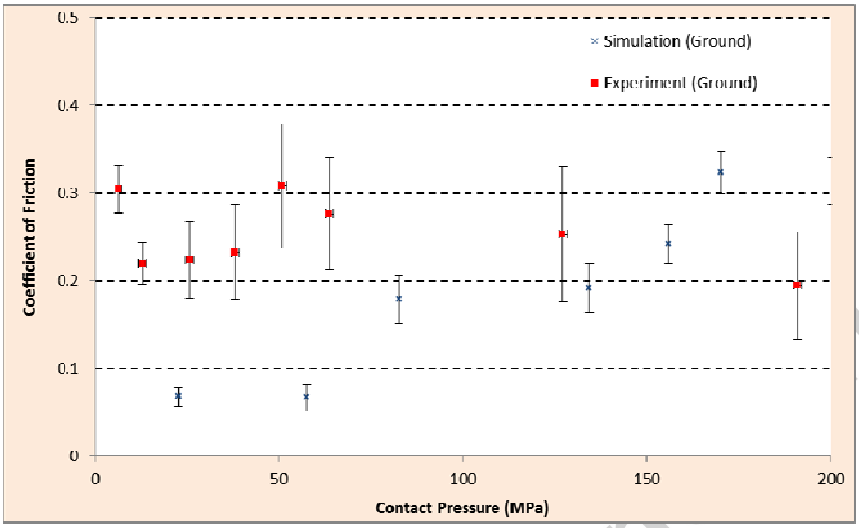

Figure 8: Simulation (DSS) and experimental results for ground surface

The agreement between simulation and experimental results is excellent in the case of polished pin (Figure 9) and the error bar from the experiment is significantly smaller due to the reduced stick-slip behaviour.

The accuracy of the model in relation to experimental results was considered better than the simulation without DSS model with the non-DSS simulation overestimated friction coefficient as illustrated in Figure 10. In addition, both experimental and simulation results with DSS for the polished surface showed a weaker trend of increasing friction coefficient with contact pressures

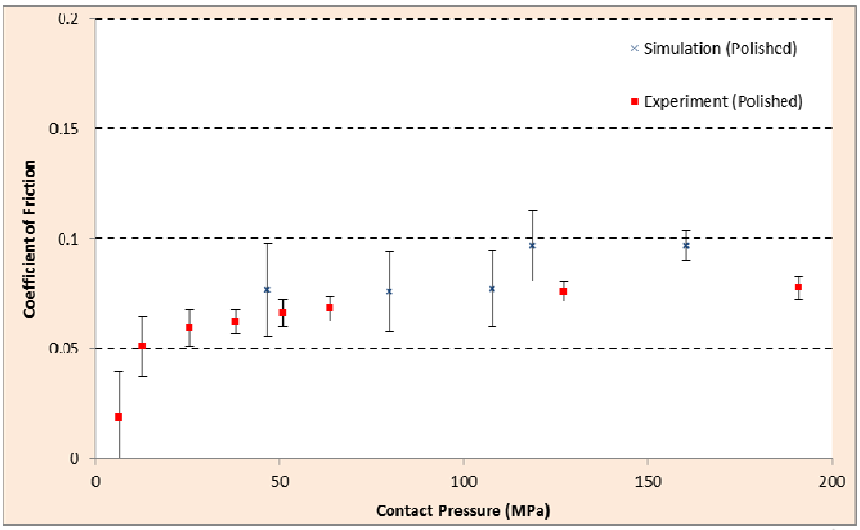

Figure 9: Simulation (DSS) and experimental results for polished surface

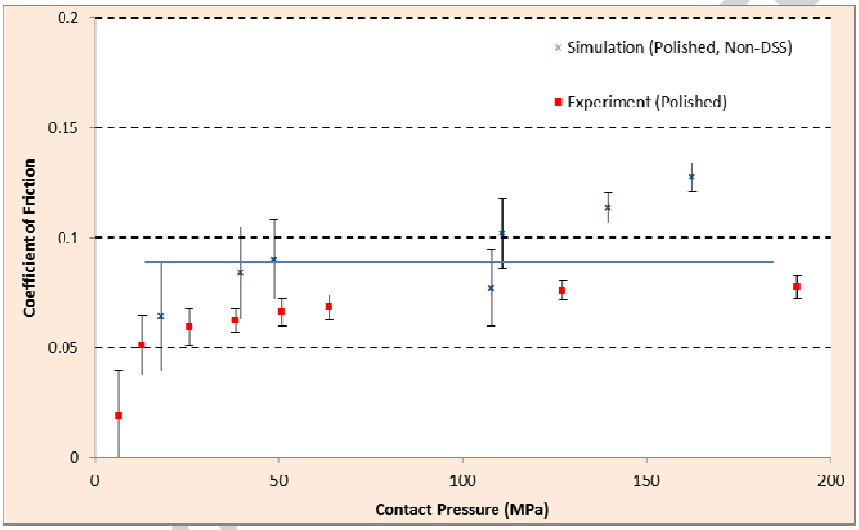

Figure 10: Simulation (non-DSS) and experimental results for polished surface

Ultimately, the DSS simulated rough surface suggests that there is no significant friction influence between tool surface with Sa 1.0and 2.5 µm as presented in Figure 11.

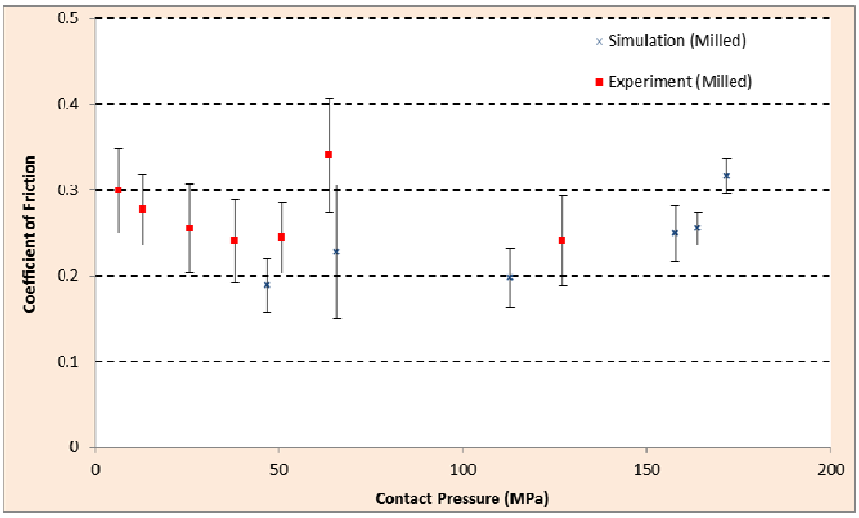

Figure 11: Simulation (DSS) results for rough surface

4 APPLICATION TO METAL FORMING SIMULATION

In order to illustrate the influence of the DSS model on a metal forming process, additional simulation on an actual metal forming geometry was performed on Deform-3D 6.9. The Deform-3D analysis code was selected because its simulation algorithm (e.g. remeshing, solution mapping) has been optimized to simulate large deformation in metal forming.

The role of finite element simulation in metal forming design has been crucial with the initial purpose of determining the suitable size and shape of metal forming preform [26, 27]. With the vast improvement in computing power over the past decade, the use of finite element method in metal forming design has extended to other purposes such as forming limit [28, 29] and springback analysis [30-32], damage prediction such as wrinkle in sheet metal forming [33] as well as non-isothermal process design [34].

The microforming T-Shape test [35] was selected as the simulation aims to identify the effect of the changing friction behaviour from DSS. The microforming T-Shape test is a

friction test designed for friction investigation in microforming. As such, it has great sensitivity to friction and is therefore very effective in demonstrating the influence of changing friction behaviour from current study on DSS mainly through the differential metal flow behaviour. The microforming T-Shape test was first introduced and developed by Taureza et al. [35, 36] and the geometry of the tested specimen (flange and total height, Figure 12) can be characterized to deduce the prevailing friction existing during the test [37].

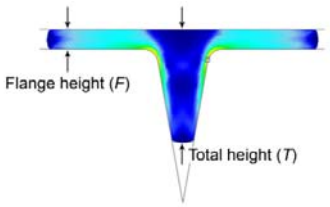

Figure 12: Friction dependent geometry in microforming T-Shape test [37]

Due to the symmetries in the microforming T-Shape test, the process simulation can be simplified by only prescribing one-quarter of the whole workpiece. The rest of the specimen can be assumed to deform in the same way to reduce the computation cost. In full, the workpiece has a starting geometry of a cylinder with 1 mm diameter and 5 mm axial length. The one-quarter workpiece –half cylinder with 2.5 mm axial length was constructed using approximately 30,000 tetrahedral elements. The mechanical properties of the workpiece used the properties definition in Figure 3.

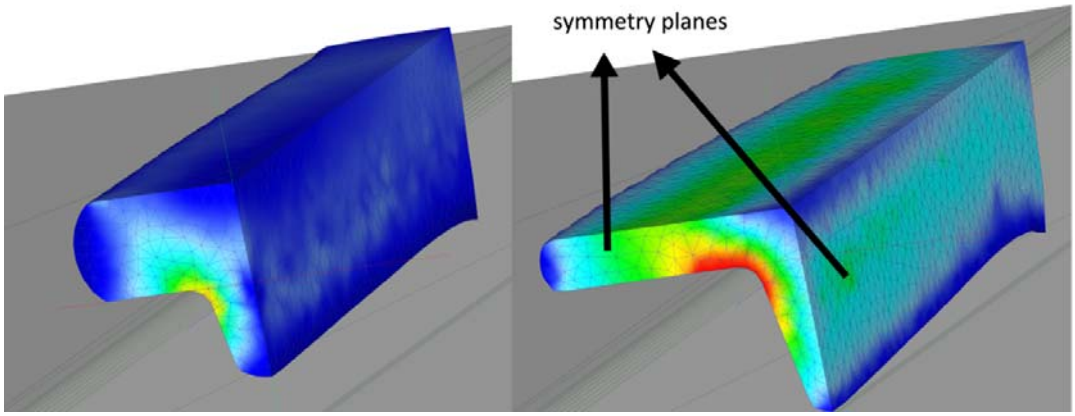

Figure 13: T-Shape simulation at 0.5 and 0.7 mm punch stroke

As for the friction definition, the Deform-3D simulation compared the two averaged friction coefficients obtained from the Abaqus simulation for the polished surface: a) with DSS model and b) without DSS model (conventional continuum simulation).

However, the current simulation is limited to contact pressure to up to 200 MPa and was focused on the shift of behaviour attributed to the addition of DSS model. For higher contact pressures, it was suggested by the work of Wanheim et al. [38] and Petersen et al. [20] that the concept of constant coefficient of friction (or Coulomb friction) does not apply in high contact pressure.

In Coulomb friction, the friction stress is proportional to the contact pressure thus yielding a constant friction coefficient. However, there is a proportionality limit to this Coulomb friction, which is further governed by the law of 'general friction' [20]. This law dictates that when the friction stress saturates when $q/2k$ exceeds 1.3with q and k correspond to the contact pressure and the yield strength of the material in pure shear, respectively. In which case, the DSS model can be applied up to contact pressure $2.6k$, beyond which the general friction (or its gradient-dependent derivative) should apply.

In the friction definition, the proportionality limit of friction stress was determined at 267 MPa of contact pressure, which corresponds to the 2.6*k* of the copper material being investigated. Hence in the Deform-3D simulation, the friction definition used was therefore reconstructed in Figure 14 with the averaged coefficient of friction from DSS simulation prescribed up to 267 MPa and the extrapolation using general friction was made for contact pressures higher than 267 MPa.

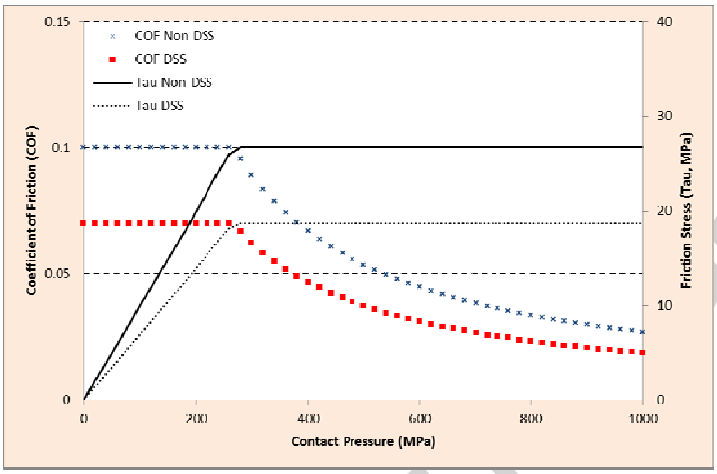

Figure 14: Friction definition used in the Deform-3D simulation

As the DSS model has been validated using tribometer experiment, the Deform-3D simulation is now aimed to demonstrate behavioural shift affected by the change of friction definition from the DSS model. As illustrated in Figure 15, when the simulation uses friction definition derived from DSS simulation, it predicts the material flow differently, i.e. lower total height at the same flange height in modified T-Shape test.

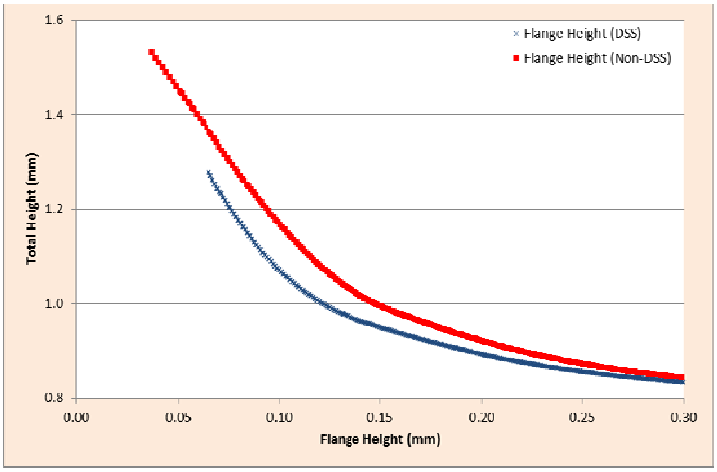

Figure 15: Change in geometry development in T-Shape test

The DSS model in general affects only the surface with the region within 3 µm from the surface having the largest effect. It was derived from hardness testing of specimens with its thickness much greater than the indentation depth. Therefore, further hardness testing experiments will help to understand the ISE behaviour when the indentation depth becomes comparable to the specimen thickness.

However, as understood in the current study, the DSS model is more accurate in predicting friction behaviour in tribometer experiment. When it is used in microforming simulation, DSS provides different metal flow prediction, which can be used to provide a size-dependent metal flow prediction, especially when the thickness of the workpiece material becomes comparable to the DSS affected depth.

5 SUMMARY

The depth-dependent stress-strain (DSS) modelling approach was developed for friction prediction simulation especially for microforming application where the shift of surface behaviour can affect the overall process behaviour significantly due to the very small

workpieces. The model was presented as an alternative to asperity simulation approach by Green which generally underestimates the amount of friction in metal to metal contact.

The current DSS model showed satisfactory agreement when it is compared with tribometer experimental results for polished and ground surfaces even without artificial implementation of friction coefficient. It is also noted that in comparison to the DSS model, the conventional continuum model overestimates friction when used with single sided asperity contact.

Ultimately, a complete metal forming simulation approach based on DSS model and a shift in metal flow preference was shown to be affected by the change of friction definition due to DSS model.

References

[1] M. Geiger, M. Kleiner, R. Eckstein, N. Tiesler, U. Engel, CIRP Annals - Manufacturing Technology, 50 (2001) 445-462.
[2] J. Jeswiet, M. Geiger, U. Engel, M. Kleiner, M. Schikorra, J. Duflou, R. Neugebauer, P. Bariani, S. Bruschi, CIRP Journal of Manufacturing Science and Technology, 1 (2008) 2-17.
[3] F. Vollertsen, Production Engineering: Research and Development, 2 (2008) 377-383.
[4] F. Vollertsen, D. Biermann, H.N. Hansen, I.S. Jawahir, K. Kuzman, CIRP Annals - Manufacturing Technology, 58 (2009) 566-587.
[5] D. Raabe, M. Sachtleber, Z. Zhao, F. Roters, S. Zaefferer, Acta Materialia, 49 (2001) 3433-3441.
[6] X. Song, S.Y. Zhang, D. Dini, A.M. Korsunsky, Computational Materials Science, 44 (2008) 131-137.
[7] R. De Borst, H.-B. Mühlhaus, International Journal for Numerical Methods in Engineering, 35 (1992) 521-539.
[8] X. Song, F. Hofmann, A.M. Korsunsky, Philosophical Magazine, 90 (2010) 3999-4011.
[9] W.D. Nix, H. Gao, Journal of the Mechanics and Physics of Solids, 46 (1998) 411-425.
[10] M. Taureza, S. Castagne, S.C.V. Lim, Key Engineering Materials, 535 (2013) 227-230.
[11] J.G. Swadener, E.P. George, G.M. Pharr, Journal of the Mechanics and Physics of Solids, 50 (2002) 681-694.
[12] N. Tymiak, D. Kramer, D. Bahr, T. Wyrobek, W. Gerberich, Acta Materialia, 49 (2001) 1021-1034.
[13] D. Chicot, Materials Science and Engineering: A, 499 (2009) 454-461.
[14] G. Feng, W.D. Nix, Scripta materialia, 51 (2004) 599-603.
[15] X. Qiu, Y. Huang, W.D. Nix, K.C. Hwang, H. Gao, Acta Materialia, 49 (2001) 3949-3958.

[16] R.K. Abu Al-Rub, Mechanics of Materials, 39 (2007) 787-802.
[17] F. Bowden, D. Tabor, Proceedings of the Royal Society of London. Series A, Mathematical and Physical Sciences, 169 (1939) 391-413.
[18] A.P. Green, Proceedings of the Royal Society of London. Series A. Mathematical and Physical Sciences, 228 (1955) 191-204.
[19] D. Mulvihill, M. Kartal, D. Nowell, D. Hills, Tribology International, 44 (2011) 1679-1694.
[20] S. Petersen, P. Martins, N. Bay, Journal of Materials Processing Technology, 66 (1997) 186-194.
[21] D. Tabor, Philosophical Magazine A, 74 (1996) 1207-1212.
[22] S. Stupkiewicz, Micromechanics of contact and interphase layers, Springer, 2007.
[23] N.P. Suh, Wear, 44 (1977) 1-16.
[24] P. Suh, Wear, 25 (1973) 111-124.
[25] M.F. Ashby, J. Abulawi, H.S. Kong, Tribology Transactions, 34 (1991) 577-587.
[26] J.J. Park, N. Rebelo, S. Kobayashi, International Journal of Machine Tool Design and Research, 23 (1983) 71-79.
[27] S.M. Hwang, S. Kobayashi, International Journal of Machine Tool Design and Research, 24 (1984) 253-266.
[28] T.B. Stoughton, International Journal of Mechanical Sciences, 42 (2000) 1-27.
[29] N. Ogawa, M. Shiomi, K. Osakada, International Journal of Machine Tools and Manufacture, 42 (2002) 607-614.
[30] K.P. Li, W.P. Carden, R.H. Wagoner, International Journal of Mechanical Sciences, 44 (2002) 103-122.
[31] F. Yoshida, T. Uemori, International Journal of Mechanical Sciences, 45 (2003) 1687-1702.
[32] W. Gan, R.H. Wagoner, International Journal of Mechanical Sciences, 46 (2004) 1097-1113.
[33] A. Makinouchi, Journal of Materials Processing Technology, 60 (1996) 19-26.
[34] S.Y. Kim, Y.T. Im, Journal of Materials Processing Technology, 127 (2002) 57-63.
[35] M. Taureza, S. Castagne, Y. Aue-u-lan, S.C.V. Lim, Journal of Materials Processing Technology, 212 (2012) 2413-2423.
[36] M. Taureza, S. Castagne, Y. Aue-u-lan, Key Engineering Materials, 447-448 (2010) 386-390.
[37] M. Taureza, X. Song, S. Castagne, Journal of Materials Processing Technology, 214 (2014) 998-1007.
[38] T. Wanheim, N. Bay, A.S. Peterson, Wear, 28 (1974) 251-258.

Highlights

- Depth-dependent stress-strain relation based on indentation size effect model is presented.
- The effect of surface roughness size effect on friction is studied.
- Tribometer experiment showed good agreement with strain gradient dependent friction simulation.

Graphical abstract